

Supporting Information for

Polythiophene - Perylene Diimide Heterojunction Field-Effect Transistors

Sreenivasa Reddy Puniredd,^{a,c} Adam Kiersnowski,^{a,b} Glauco Battagliarin,^a Wojciech Zajączkowski,^a Wallace W. H. Wong,^c Nigel Kirby,^d Klaus Müllen^{*,a} and Wojciech Pisula,^{*,a,f}

^a Max Planck Institute for Polymer Research, Ackermannweg 10, 55128 Mainz (Germany).

^b Wrocław University of Technology, Polymer Engineering & Technology Division, Wybrzeże Wyspiańskiego 27, 50-370 Wrocław, Poland

^c School of Chemistry, Bio21 Institute, University of Melbourne, 30 45 Flemington Road, Parkville, Victoria 3010, Australia

^d Australian Synchrotron, 800 Blackburn Road, Clayton, Victoria 3168, 50 Australia

Corresponding Authors

* pisula@mpip-mainz.mpg.de
muellen@mpip-mainz.mpg.de

present addresses:

^e Institute of Materials Research and Engineering, A*Star, 3 Research Link, Singapore, 117602

^f Evonik Industries AG, Kirschenallee, 64293 Darmstadt, Germany

Experimental

P3HT (BASF SE Sepiolid™ P100 with a regioregularity of ~94%, Mw=60 kg/mol and PDI=2.2), PDI-1¹ and PDI-2 were separately dissolved in chloroform at a concentration of 10 mg/ml and stirred for 12 h at 30 °C. The solutions were then mixed and further stirred for 1 h at 30 °C to make the blends of different weight ratios. Prior to deposition the solution of P3HT:PDI blends were filtered through a PTFE syringe filter (0.45 µm pore size). The pure and blended solutions were then spin-coated on top of the hexamethyldisilazane (HMDS) treated bottom contact FET surface at 1200 rpm for 1 min yielding a film thickness of ~ 100 nm. The films were annealed at 120 °C for 20 min on a hot plate in the glove box. We have prepared the films on HMDS treated FET surface with pure P3HT, PDI-1 and PDI-2 and also blends of 1:1,1:3 and 3:1, (w/w) of P3HT:PDI-1 and P3HT:PDI-2, respectively. FET measurements were recorded after annealing the samples. All the above procedures and FET

measurements (using a Keithley 4200 semiconductor parameter analyzer) were carried out inside a dry nitrogen glovebox. These devices were also used for all other characterizations.

Bottom gate/bottom contact FETs were fabricated using a heavily doped silicon wafer as the gate electrode with a 230 nm thick layer of thermally grown SiO₂ functioning as the gate dielectric (capacitance = 14.6 nFcm⁻²). The source and drain electrodes consist of 10 nm of high work function (ITO) adhesive layer coated with 30 nm of Au. An interdigitated electrode configuration with typical length $L = 5\text{--}20\ \mu\text{m}$ and width $W = 10\ 000\ \mu\text{m}$ ($W L^{-1} = 500\text{--}4000$) was used. The silicon oxide surface was treated with HMDS (hexamethyldisilazane) to form a hydrophobic monolayer.

Using standard FET analysis, quantitative carrier mobilities (μ) can be calculated in the saturation regime by the following relationship:

$$I_{DS} = \frac{WC_i\mu}{2L}(V_{GS} - V_T)^2$$

where C_i is the capacitance per unit area of the SiO₂ is gate dielectric and V_T is the threshold voltage.

Atomic force microscopy (AFM) images of the pure PDI, P3HT molecules and also the blends active layer were recorded with a Multimode phase AFM NanoScope IV Scanning Probe microscope controller functioning in tapping mode.

Cross sectional SEM images of the blends were carried out with Zeiss Gemini 1530 and also Hitachi SU8000.

GIWAXS measurements were performed using a custom setup consisting of rotating anode X-ray source (Rigaku Micromax, operated at 42kV and 20mA), Osmic confocal MaxFlux optics and a three pin-hole collimation system (JJ X-ray). Samples on the top of 1×1 cm silicon substrates were irradiated at the incident angle (α_i) of 0.20°. Diffraction patterns were recorded for 3h on a MAR345 image plate detector. The camera length (315 mm, calibrated using silver behenate) and the diameter of the detector (34.5 cm). Finally, the data was processed using Datasqueeze 2.2.5 program.

Temperature dependent GIWAXS measurements of P3HT were performed on the Australian Synchrotron SAXS/WAXS beamline at a wavelength of 0.6888 Å. The spot size on the sample was 250 (H) x 80 (V) μm FWHM. The height and zero incident angle was calibrated for each individual sample, then data collected at an incident angle of 0.18° using a MAR165 CCD detector at a distance of 391 mm from the sample with a vacuum path between the sample and detector. A custom built heating stage for the samples was used for these in-situ heating measurements which were performed in air atmosphere. The samples were heated at a

rate of ca 10 ° C/min to the desired temperature with subsequent equilibration at each temperature for ca 2 min before the collection of data.

Results

Field-effect transistors

Table S1. FET charge carrier mobility (μ) error and threshold voltage (V_T) for pure P3HT, PDI-1 and PDI-2 and blends of P3HT:PDI-1 and P3HT:PDI-2.

Sample	$\mu_{h,sat}$ (cm ² /Vs)	$V_{T\ holes}$ (V)	$\mu_{e,sat}$ (cm ² /Vs)	$V_{T\ electrons}$ (V)
P3HT	$3.7\pm 1.5\times 10^{-2}$	~ 5	-	-
PDI-1	-	-	$3\pm 2\times 10^{-6}$	-*
1:3 P3HT:PDI-1	$1\pm 0.3\times 10^{-3}$	~ -10	-	-
1:1 P3HT:PDI-1	$4.5\pm 2\times 10^{-3}$	~ -25	$6\pm 2\times 10^{-3}$	~ 20
3:1 P3HT:PDI-1	$3\pm 1.5\times 10^{-3}$	~ -20	$2\pm 0.5\times 10^{-5}$	~ 30
PDI-2	-	-	$5\pm 2\times 10^{-8}$	-*
1:3 P3HT:PDI-2	$7\pm 2\times 10^{-3}$	~ -10	$2\pm 0.8\times 10^{-3}$	~ 40
1:1 P3HT:PDI-2	$3\pm 1.5\times 10^{-3}$	~ -0	-	-
3:1 P3HT:PDI-2	0.1 ± 0.03	~ -5	-	-

* V_T is not assignable for both PDI derivatives.

Integrations of GIWAXS patterns

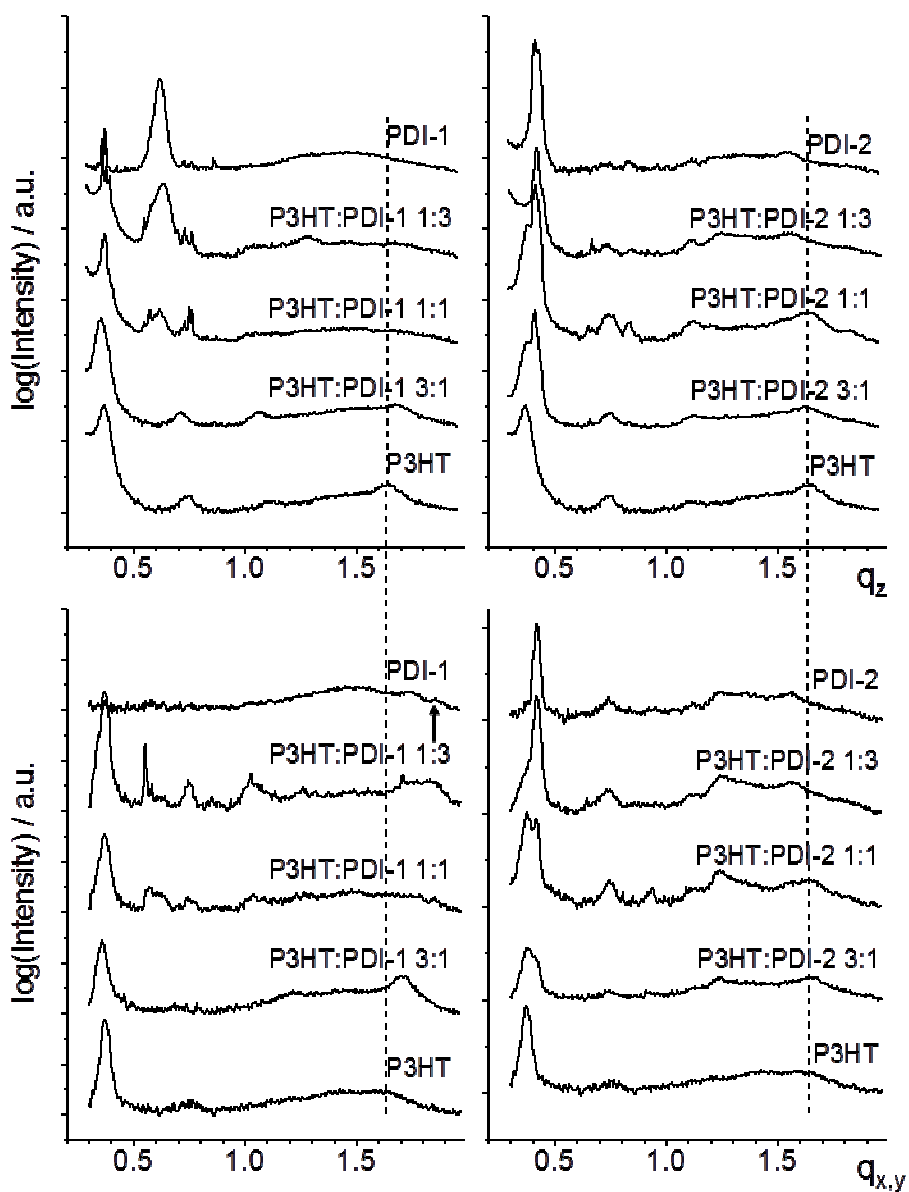


Figure S1. Equatorial (along $q_{x,y}$ at $q_z = 0 \text{ \AA}^{-1}$) and meridional (along q_z at $q_{x,y} = 0 \text{ \AA}^{-1}$) integrations of the GIWAXS patterns for thin films of P3HT, PDI-1 and PDI-2 and the corresponding blends. Dashed line indicates the position of the π -stacking reflection of pure P3HT, the π -stacking peak for PDI-1 is labeled by an arrow.

Annealing effect of P3HT

Additional temperature dependent in-situ GIWAXS measurements were performed at the Australian Synchrotron, Melbourne, to monitor structural changes in P3HT during heating and cooling. To investigate the annealing effect, the meridional π -stacking reflection was analyzed by plotting the full width at half maximum (FWHM) of the radial (ξ) and azimuthal (Ψ) peak distribution as a function of temperature (Figure 3). While, according to the Scherrer's law, ξ is inversely proportional to the coherence length of molecules within the stack, the Ψ directly shows the angular distribution of aromatic planes within the domains. In general, smaller ξ and Ψ values indicate larger sizes of ordered domains and higher anisotropy. Interestingly, ξ and Ψ follow an identical trend during heating the P3HT film. After a minor growth, the values gradually decrease toward 120 °C and remain almost unchanged after cooling back the sample down to room temperature. This result clearly indicates that thermal annealing enhances both coherence of macromolecules within stacks (in other words: longer coherence length) and also ordering of stacks in respect to the surface the surface. It has to be noted that during this procedure the sample has not been melted as performed in a previous report on P3HT and P3HT:PCBM mixtures.²

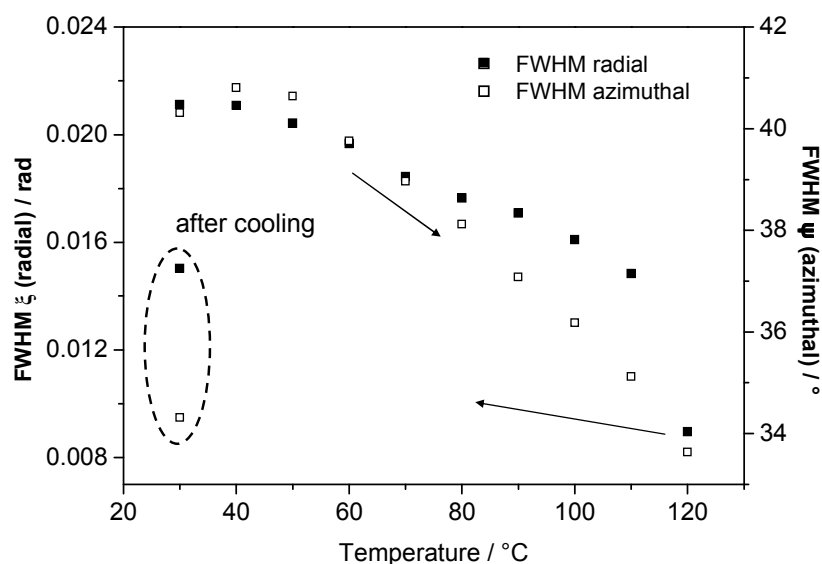


Figure S2. The FWHM of the π -stacking reflection of P3HT thin film in the radial (along q_z at $q_{x,y} = 0 \text{ \AA}^{-1}$) and azimuthal directions determined from in-situ GIWAXS measurements at different temperatures. Arrows indicate the heating/cooling direction.

Microstructure of P3HT:PDI-2

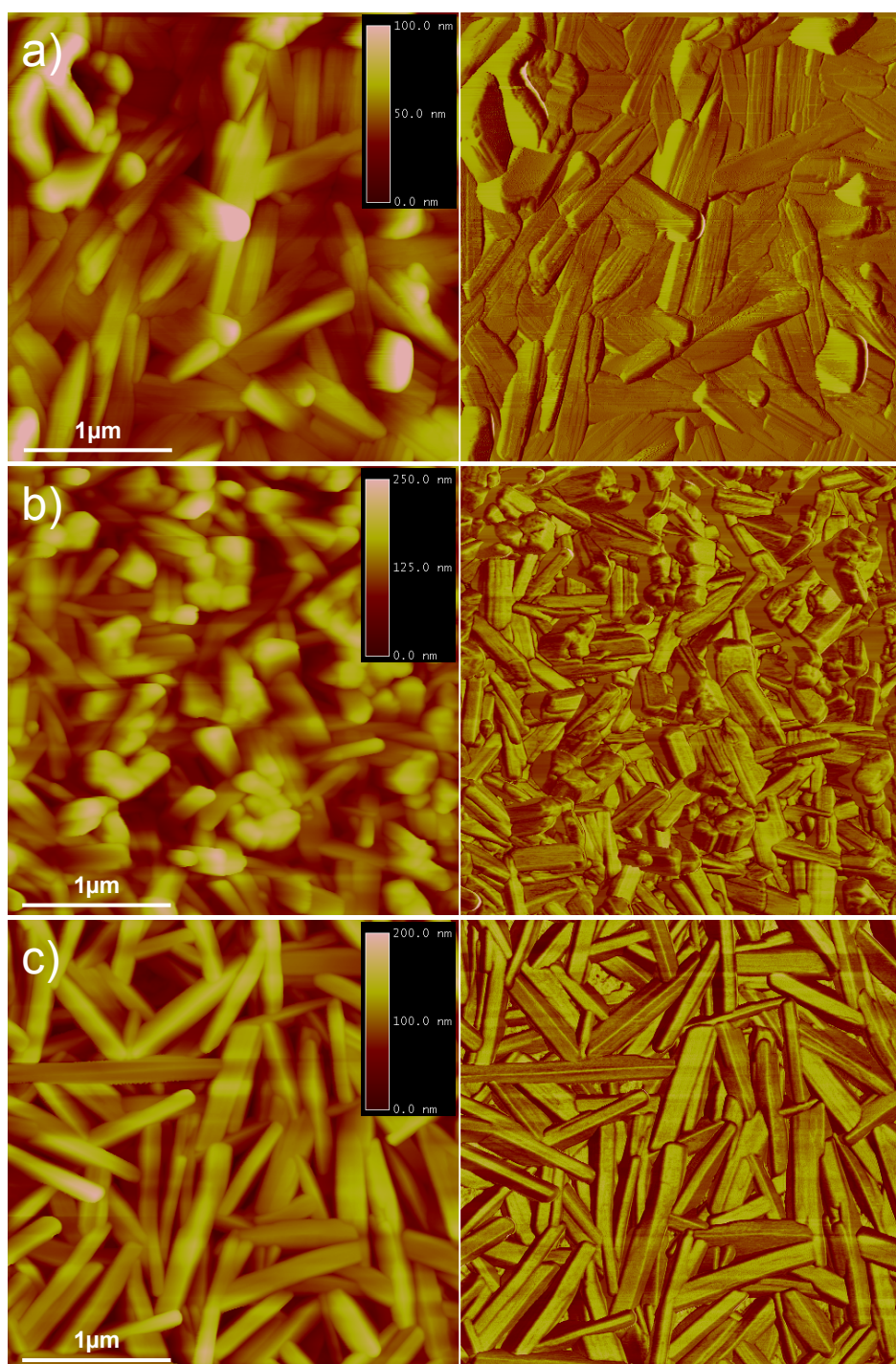


Figure S3. AFM height (left) and phase (right) images for P3HT:PDI-2 blend films with the weight ratios of a) 1:3, b) 1:1, and c) 3:1.

¹ Synthesized according to Y. Yang, Y. Wang, Y. Xie, T. Xiong, Z. Yuan, Y. Zhang, S. Qian, Y. Xiao, *Chem. Commun.* 2011, **47**, 10749.

² E. Verploegen, R. Mondal, C. J. Bettinger, S. Sok, M. F. Toney, Z. Bao, *Adv. Funct. Mater.* 2010, **20**, 3519.